Electron Photodetachment from Aliphatic Molecular Anions. Gas-Phase Electron Affinities of Methoxyl, *tert*-Butoxyl, and Neopentoxyl Radicals

Bruce K. Janousek, Albert H. Zimmerman, Kenneth J. Reed, and John I. Brauman*

Contribution from the Department of Chemistry, Stanford University, Stanford, California 94305. *Received March 21, 1977*

Abstract: The cross section for electron photodetachment has been measured for methoxyl, *tert*-butoxyl, and neopentoxyl anions using an ion cyclotron resonance spectrometer in conjunction with a xenon arc lamp. Cross sections for *tert*-butoxyl and neopentoxyl anions were also measured at high resolution with a tunable dye laser. Cross section shapes near threshold are calculated and compared to the low- and high-resolution results. The high-resolution cross sections show fine structure as a result of photodetachment to excited vibrational states of the product neutrals. The gas-phase electron affinities are determined to be EA(CH_3O) = 1.59 ± 0.04 eV, EA((CH_3)$_3$CO) = 1.87 ± 0.01 or 1.90 ± 0.01 eV, and EA((CH_3)$_3$$CCH_2O$) = 1.93 ± 0.05 eV (36.7 ± 0.9, 43.1 ± 0.2 or 43.8 ± 0.2, and 44.5 ± 1.4 kcal/mol, respectively). Substituent effects on alkoxyl anion stability are discussed in terms of a perturbation model which appears to be useful in predicting electron affinity trends.

Introduction

Electron photodetachment spectroscopy is one of the most useful methods available for determining the spectroscopic properties of negative ions. This technique may be used to measure the dependence of the cross section on photon energy for the process

$$A^- + \hbar\omega \rightarrow A + e^- \quad (1)$$

For molecular negative ions these experiments can provide information on molecular geometries, vibrational frequencies, and spin–orbit coupling constants.[1-5] Photodetachment experiments also provide a means of determining electron affinities of both atomic and polyatomic species. The electron affinity of A is the minimum energy required to remove an electron from A^- where A^- and A are in their ground rotational, vibrational, and electronic states and the detached electron has zero kinetic energy. While electron affinities of atoms and small molecules may usually be obtained from photodetachment cross sections,[6,7] for larger molecules the interpretation of the cross section is often complicated by the wealth of spectroscopic information contained therein.[8] The problems in interpreting these experiments typically arise in first resolving and then identifying the numerous allowed vibronic transitions.

In this paper we report the measured photodetachment cross sections for methoxyl, *tert*-butoxyl, and neopentoxyl anions. This work is an extension of an earlier publication on alkoxyl anions.[9] In the present paper, we utilize a high-resolution (<1 Å) dye laser as a light source for the photodetachment of the *tert*-butoxyl and neopentoxyl anions. The resulting cross sections are qualitatively similar to those observed with low resolution; the high-resolution cross sections, however, exhibit progressions of vibronic transitions. The adiabatic electron affinity of the *tert*-butoxyl radical is determined by a qualitative Franck–Condon analysis which assumes that the ions in the ICR cell are thermalized.

The trend in the electron affinities of the alkoxyl radicals may be correlated with the effects of alkyl groups on anion stability. We present a perturbation molecular orbital model which accounts for the observed stability of the alkoxyl anions.

Experimental Section

A. Instrumental. The photodetachment experiments were performed on a Varian V-5900 ion cyclotron resonance spectrometer with a modified square cell design.[10,11] Satisfactory photodetachment data were obtained by employing high trapping potentials (1.5–3.0 cV), low analyzer (<0.3 eV), and moderate source drift (<1.0 eV) potentials. For the relatively low molecular weight methoxyl anion, doubling both the magnetic field to 6.2 kG and ω_1 to 307.14 kHz resulted in much improved trapping times and consequently better photodetachment signals. Experiments on each ion were performed in the pressure range 0.3–8.0 × 10^{-6} Torr with the exception of neopentyl alcohol, where lower pressures (~0.2 × 10^{-6} Torr) gave the best results.[12]

The 1000-W xenon arc lamp and grating monochromator employed in the low-resolution studies have been previously described.[10,11] Experiments on *tert*-butoxyl anion were performed with a resolution of 13.2 and 23.8 nm (fwhm) while a resolution of 23.8 nm was obtained on the other ions. Calibrations of the visible grating (blazed at 600 nm) before and after these experiments were consistent to ±1 nm.

The light source used in the high-resolution experiments consisted of a Coherent Radiation Model 590 dye laser pumped with a Coherent Radiation Model CR-12 argon ion laser. The dyes employed in these studies were rhodamine 110 (540–600 nm), rhodamine 6G (570–655 nm), rhodamine B (610–655 nm), and rhodamine 640 (645–690 nm). The dyes were normally pumped with about 4 W from the visible argon lines. Several milliliters of cyclooctatetraene were added to each dye solution to act as a triplet quencher and increase the dye laser output power. A typical experiment employed output powers of 50–400 mW and a line width of <1 Å. In order to prevent spatial inhomogeneity of ions in the cell from producing spurious results, the laser beam was expanded to approximately the diameter of the cell window (about 2 cm). At each wavelength, approximately 4% of the beam was split off and directed into an Epply thermopile, from which the relative output power was recorded. After each run, the wavelength of the dye laser output was calibrated to ±3 Å against a Beck wavelength reversion spectroscope.

In both the low- and high-resolution experiments, displays of the full negative ion signals with and without light revealed no spurious frequency shifts or production of other ions.

B. Anion Generation. A direct and facile method for generating alkoxyl anions is low-energy electron impact on dialkyl peroxides. Dimethyl peroxide was synthesized by the method of Hanst and Calvert[13] via methylation of hydrogen peroxide. Electron impact at 0.6–0.8 eV above trapping on the twice distilled (at −23 °C) product afforded CH_3O^- exclusively. Degassed di-*tert*-butyl peroxide (Matheson Coleman and Bell) gave ions of *m/e* 73 ((CH_3)$_3$$CO^-$) and 57 (presumably the enolate $CH_3COCH_2^-$ which may arise from acetone via loss of CH_3· from *tert*-butoxyl radical[14]) using an electron beam energy of ~4.0 eV. Photodetachment of the *m/e* 73 ion could be studied independently of the *m/e* 57 ions since ejection studies revealed that the former ion is the precursor to the enolate.

Thynne[15] has established that electron impact on aliphatic alcohols produces alkoxyl ions and not carbanions. At the lowest dissociative capture maximum of *tert*-butyl alcohol (MCB), 5.5 eV, double resonance showed that the *m/e* 73 anion, *tert*-butoxyl, is formed as the result of proton transfer to H^-.[16] At its second dissociative capture

0002-7863/78/1500-6142$01.00/0

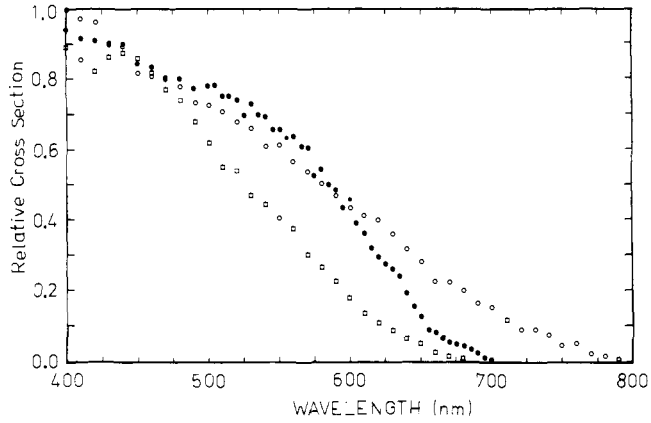

Figure 1. Photodetachment cross sections of methoxyl (○), *tert*-butoxyl (●), and neopentoxyl (□) anions determined at a resolution of 23.8 nm (fwhm).

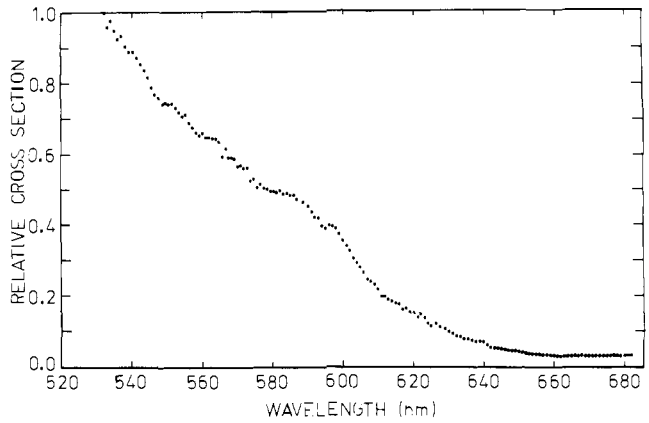

Figure 2. Laser photodetachment cross section of neopentoxyl anion (resolution < 1 Å).

peak, 9.0 eV, photodetachment of *tert*-butoxyl anion was studied free of H^- interference.

We have demonstrated[9] that proton transfer to fluoride ion (produced from NF_3) is a convenient source of secondary anions. For methanol, this reaction has a $\Delta G°_{298}$ of +6.2 kcal/mol[17] and is not observed. For *tert*-butyl alcohol, the reaction is slightly endothermic ($\Delta G°_{298}$ = +0.8 kcal/mol)[17] but proved[9] to be a good source of *tert*-butoxyl ion, $k = (0.9 \pm 0.2) \times 10^{-10}$ cm^3 molecule^{-1} s^{-1}. The amount of *tert*-butoxyl ion produced by this reaction could be increased by increasing the translational energy of the fluoride ion with a double resonance oscillator.[18] The reaction of F^- with neopentyl alcohol is slightly exothermic ($\Delta G°_{298}$ = −0.5 kcal/mol)[17] and fast[9] ($k = 2.2 \pm 0.4 \times 10^{-10}$ cm^3 molecule^{-1} s^{-1}). Secondary ions generated by this method have been established as alkoxyl ions from experiments on deuterated compounds.[19] No additional methods for producing neopentoxyl ion were employed.

C. Data Analysis. Techniques for data acquisition and analysis have been previously described.[10,11,20] Comparison of the flow model treated by Smyth and Brauman[10,11] and the steady-state model[21] showed that both descriptions of ion behavior gave essentially identical results for fractional signal decreases less than ~0.50. When the fractional decreases were larger than this, the steady-state model provided the best description of ion behavior.

Results

The relative photodetachment cross sections at low resolution for methoxyl, *tert*-butoxyl, and neopentoxyl anions are shown in Figure 1. The data for *tert*-butoxyl anion were obtained for anions generated by proton abstraction from *tert*-butyl alcohol by F^-. Similar results were obtained for *tert*-butoxyl anions generated by dissociative electron impact on di-*tert*-butyl peroxide.[9] Attempts to study the photodetachment of ethoxide ion *m/e* 45 (produced from diethyl peroxide) were unsuccessful, since its lifetime is limited by a reaction producing ion *m/e* 43. This ion has been identified from its photodetachment spectrum as the enolate of acetaldehyde.[22] Its production may be a consequence of peroxide pyrolysis at the hot filament. This appears to be characteristic of starting materials possessing β hydrogens and has been observed previously.[23]

The relative photodetachment cross sections at high resolution for neopentoxyl and *tert*-butoxyl anions are shown in Figures 2 and 3, respectively. The *tert*-butoxyl anions were formed by either proton abstraction from *tert*-butyl alcohol by F^- or dissociative electron impact of di-*tert*-butyl peroxide. The results were identical in each case.

In order to make any changes in slope more obvious in these high-resolution spectra, the curves have been fit to a series of cubic splines and these splines have been differentiated. The derivative of the smoothed spline curve for the *tert*-butoxyl cross section is given in Figure 3 with the original cross section (see below).

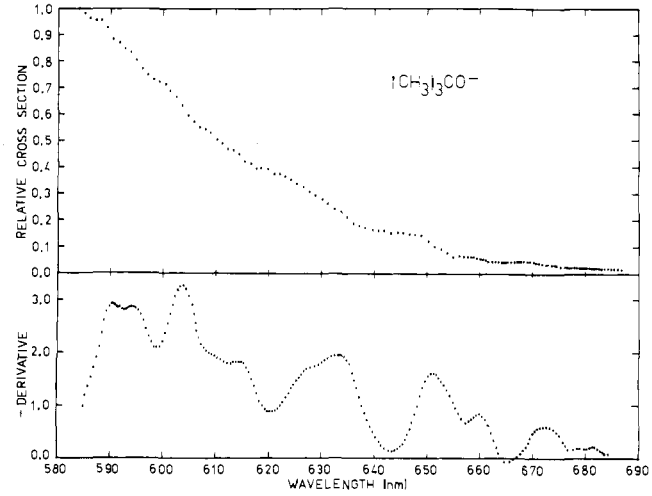

Figure 3. Laser photodetachment cross section of *tert*-butoxyl anion and smoothed derivative of the observed cross section.

Splines

Given a set of data points, $(x_0,y_0)\cdots(x_n,y_n)$, a spline, $S(x)$, is an interpolating function which consists of a series of connected cubic polynomials satisfying the conditions that (1) $S(x)$ goes through all the data points; (2)

$$\int_{x_0}^{x_n} [S''(x)]^2 dx$$

is minimized; and (3) adjacent cubic polynomials join continuously with continuous first and second derivatives. The function satisfying these criteria is unique and possesses the minimum curvature property, i.e., the cubic spline is the smoothest function which passes through all the data.

To smooth the data of random noise, we have employed the routine developed by Reinsch.[24] This technique approximates the data by a cubic spline determined by least squares. Thus, this spline does not necessarily pass through the y_i's, but is near to them in the following sense.

Given the set of all twice continuously differentiable functions g defined on $[x_0,x_n]$ with

$$\sum_{i=0}^{n} \left[\frac{g(x_i) - y_i}{\delta y_i}\right]^2 \leq P \qquad (2)$$

the spline found by the Reinsch routine is smoothest in that

$$\int_{x_0}^{x_n} [S''(x)]^2 dx \leq \int_{x_0}^{x_n} [g''(x)]^2 dx \qquad (3)$$

for all g. The δy_i estimate the accuracy of the data and P is a parameter which determines the amount of smoothing. For P

= 0, the spline goes through all the data points and no smoothing is done. As P is increased, the difference between the data point, y_i, and the smoothed spline, $S(x_i)$, is increased. This difference, the residual, R_i, is thus defined by

$$R_i = y_i - S(x_i) \tag{4}$$

By multiplying adjacent residuals and summing over these products, we obtain a normalized correlation function Q defined as

$$Q = \sum_i \frac{R_i R_{i+1}}{R_i^2} \tag{5}$$

which is a measure of the amount of smoothing. For large P, the spline approaches a straight line and adjacent data points are mostly on the *same* side of the smoothed curve giving rise to a positive value of Q. For small P (little smoothing) adjacent data points tend to be on *opposite* sides of the smoothed curve and Q is negative (anti-correlated). In practice, Q varies smoothly with P and we take the value of P for which $Q = 0$ to represent the amount of smoothing that eliminates random noise in the data.

Discussion

A. Threshold Laws. Understanding how the electronic photodetachment transition varies with energy near threshold is critical in the interpretation of molecular photodetachment cross sections. The changes in slope of the cross sections in Figures 2 and 3 indicate that the cross section for each vibronic transition shows an abrupt increase at its threshold. However, since the cross section represents the superposition of a number of transitions of varying intensity, it is difficult to obtain quantitative information from the experimental data on how the electronic transition moment depends on energy. Thus, it is important to have some a priori knowledge of the photodetachment cross section behavior as a tool in interpreting experimental cross section.

The threshold energy dependence of a collision cross section for a process which has two product particles depends only on the long-range forces between the products.[25] For photodetachment from anions the departing photoelectron interacts with the neutral through a weak potential which falls off faster than r^{-2} (neglecting charge-dipole interaction between the electron and the neutral). For this case the cross section for the production of two particles with angular momentum $l\hbar$ with respect to their common center of mass is given near threshold by

$$\sigma \propto E_k^{\,l+1/2} \tag{6}$$

where E_k is the energy of the ejected electron. The behavior of the cross section at threshold is determined by the lowest allowed value of the photoelectron angular momentum (l). This value is easily determined from the symmetry of the anion by the application of group theory.[26]

The simplest theoretical model of photodetachment is a one-electron transition from a bound orbital of the anion to a free electron continuum state. Using first-order time-dependent perturbation theory one finds the cross section to be proportional to the square of the dipole matrix element of the bound and continuum states. For a given symmetry of the anion bound state, dipole selection rules may be used to determine the lowest order partial wave for the detached electron. We may then extend eq 6 by expanding σ in terms of partial cross sections $\sigma_l(E)$ to give[26]

$$\sigma(E_k) = \sum_{l^*=0}^{\infty} A_{l^*} E_k^{\,l^*+1/2}[1 + O(E_k)] \tag{7}$$

E_k is the energy above threshold and l^* is the smallest value of l for which $\sigma_l(E)$ is not identically zero due to symmetry. The value of l^* can be determined from the selection rule $\Delta l = \pm 1$ and group theory. The initial state for the photodetachment process may be regarded as the highest occupied molecular orbital (HOMO) of the anion. This orbital can be assigned some characteristic value of l. For example, for species of C_{3v} symmetry such as methoxyl and *tert*-butoxyl anions the HOMO will have E symmetry. Since the E representation transforms as x or y in the C_{3v} point group the HOMO has $l = 1$ and the selection rule $\Delta l = \pm 1$ gives $l^* = 0$. Therefore, from eq 6,

$$\sigma \propto E_k^{\,1/2} \tag{8}$$

at threshold which results in a cross section that rises with infinite slope. For neopentoxyl anion, the HOMO possess A″ symmetry in the point group C_s which also gives an $E_k^{\,1/2}$ dependence for the cross section at threshold.

To determine the energy dependence of the cross section above threshold quantitatively we must extend the group theoretical model. In previous work we have shown that photodetachment cross sections may be calculated near threshold using HOMO initial states obtained from molecular orbital calculations[27] on the anions, and partially orthogonalized plane wave (POPW) final states.[26] The HOMO initial states are (using CNDO/2)

$$\psi_{MeO} = 0.3369\phi_s(H_2) - 0.3489\phi_s(H_3) - 0.8717\phi_{p_y}(O) \tag{9}$$

$$\psi_{t\text{-}BuO} = 0.1389\phi_s(C_2) + 0.1059\phi_{p_x}(C_2) - 0.2020\phi_{p_y}(C_2) + 0.1076\phi_{p_z}(C_3) - 0.1389\phi_s(C_3) - 0.1059\phi_{p_x}(C_3) - 0.2020\phi_{p_y}(C_3) - 0.1076\phi_{p_z}(C_3) + 0.1557\phi_{p_y}(C_4) - 0.8892\phi_{p_y}(O) \tag{10}$$

$$\psi_{neopentO} = 0.1698\phi_s(H_{10}) + 0.1698\phi_s(H_{11}) - 0.1355\phi_s(C_4) - 0.2990\phi_{p_z}(C_4) + 0.1315\phi_{p_z}(C_5) - 0.8466\phi_{p_z}(O) - 0.2644\phi_{p_x}(O) \tag{11}$$

The doubly degenerate orbitals for methoxyl and *tert*-butoxyl anions give identical cross sections; thus, only one of each degenerate pair is given above. The numbering scheme of the atoms used in these calculations is given below where the x-z plane was taken to be the plane of the paper.

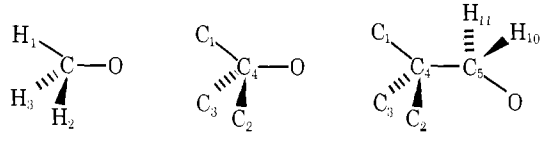

1 2 3

We have found that to calculate photodetachment cross sections accurately the radial diffuseness of the HOMO must be increased over that for a neutral molecule. This is reasonable since there is substantial evidence that the outermost orbitals of negative ions are much more diffuse than those in neutral compounds.[28] We have used the orbital exponents for Slater-type orbitals which best describe the atomic photodetachment cross sections for each atomic species. These orbital exponents follow: hydrogen, 0.32 au^{-1}; carbon, 0.56 au^{-1}; and oxygen, 0.68 au^{-1}.

Using HOMO initial states and POPW final states the dipole matrix element of the transition is calculated and the cross section is obtained as a function of energy. The details of this calculation have been previously described.[26] The calculated cross sections are plotted vs. E_k in Figure 4 for the three alkoxyl anions. The photodetachment cross section similarly calculated for O^- is shown for comparison.

The most important feature of the alkoxyl anion cross sections shown in Figure 4 is that they all rise quite sharply at threshold. This behavior is similar to that of O^- and is a result

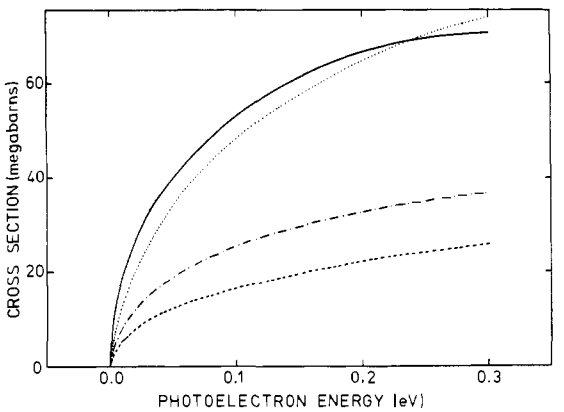

Figure 4. Calculated photodetachment cross sections for O^- (- · · · -), CH_3O^- (- - - -), $(CH_3)_3CO^-$ (—), and $(CH_3)_3CCH_2O^-$ (· · · · ·).

of the s waves at threshold. However, at energies above threshold the presence of the alkyl group introduces a significant effect. In the case of methoxyl and neopentoxyl anions substantial electron density in the HOMO is delocalized from oxygen onto the hydrogen atoms. Inspection of the wave functions for these HOMOs shows that they have significant π^* character and thus should show behavior similar to, for example, O_2^-. That is, the cross section continues to rise far above threshold and looks like that for a p wave ($l = 1$).[29] The *tert*-butoxyl anion has a HOMO with more electron density on the oxygen, and has a cross section which levels off in a manner more similar to that of O^-.

In systems such as alkoxyl anions where both s and p waves are symmetry allowed, an intuitively simple picture of the cross section is obtained from eq 7. The molecular symmetry tells us that both $l^* = 0$ and $l^* = 1$ are allowed and, therefore, that both A_0 and A_1 will be nonzero to first order. The relative magnitudes of the nonzero coefficients in the case of the alkoxyl anions are determined by the type and extent of electron delocalization. For example, electron delocalization into hydrogen s orbitals increases A_1 relative to A_0, resulting in cross sections which continue to rise after an initial sharp rise at threshold. These considerations indicate that the photodetachment cross section is a sensitive probe of delocalization of the outermost electron in a negative ion.

B. Vibronic Transitions. The principal problem in comparing theoretical cross sections with our experimental results is that the Franck-Condon overlaps between the vibrational levels in the anion and product neutral are difficult to estimate for molecules of this complexity. In fact, the experimental cross sections in Figure 1 do not rise with infinite slope at threshold but rise linearly, suggesting that the cross section contains a number of closely spaced vibronic transitions to excited vibrational states of the product neutral. The appearance of these vibronic transitions in the high-resolution cross section is further evidence that off-diagonal Franck-Condon factors are spreading the photodetachment transition probability over a large region (~150 nm). To a first approximation, the height of a peak in the derivative of the smoothed splines of *tert*-butoxyl and neopentoxyl can be taken to be proportional to the intensity of the vibronic transition giving rise to that peak. The results of such an analysis for *tert*-butoxyl anion are given in Table I. We have made no effort to assign these transitions since we do not have enough data to make a meaningful or unique vibronic assignment.

In an effort to obtain a qualitative picture of the Franck-Condon overlaps in the photodetachment of CH_3O^-, we have done a CNDO/2 optimization of the geometry of methoxyl anion and radical, the results of which are given in Table II. The changes in geometry between anion and radical are in excellent agreement with those calculated by Yarkony et al.[30]

Table I. Positions and Relative Intensities of Vibronic Transition Observed in the Photodetachment of *tert*-Butoxyl Anion

wavelength, nm	rel intensity	wavelength, nm	rel intensity
592.5	0.74	636.0	1.19
596.5	1.20	652.5	1.03
606.0	1.86	661.5	0.47
617.0	0.87	675.0	0.42
631.0	0.48		

Table II. Optimized CNDO/2 Geometries

molecule	state	r_{CO}, Å	r_{CH}, Å	MeCMe angle* or HCH angle, deg	θ,[a] deg
CH_3O^-	$\tilde{X}^1A_1$	1.33	1.15	102.9	0
$CH_3O\cdot$	$\tilde{X}^2E$	1.35	1.12	109.1	3.9
t-BuO$^-$	$\tilde{X}^1A_1$			109*	0
t-BuO·	$\tilde{X}^2E$			113*	7

[a] θ is the angle between the C_{3v} axis and the equilibrium position of the oxygen atom.

(ab initio SCF with double-ζ basis set). The increase in the HCH angle in going to the neutral suggests that the umbrella-like bending mode in the methoxyl system will have large off-diagonal Franck-Condon factors. We have also done a partial geometry optimization (CNDO/2) on *tert*-butoxyl anion and radical giving the results shown in Table II. Analogous to the methoxyl case, the MeCMe angle increases in going to the neutral. Both methoxyl and *tert*-butoxyl radicals are predicted to undergo a Jahn-Teller distortion which will move the C-O bond off the threefold symmetry axis (Table II).[31] This interaction will likewise be responsible for an increase in the off-diagonal Franck-Condon overlaps in the two systems and could give rise to irregular vibrational progressions in the photodetachment spectrum.

C. Electron Affinities. In order to turn the above spectroscopic results into thermochemical information (i.e., electron affinities) we must assign the $A^-(v'' = 0,0,0, \ldots) \rightarrow A\cdot(v' = 0,0,0, \ldots)$ transition to the photodetachment spectra. This assignment will depend upon the assumed vibrational temperature of the ions in the ICR cell. Typically, we expect the ions in the ICR cell to have a vibrational temperature near 300 K since the ~1 s trapping times should allow the ions to release most of any excess vibrational energy via collisions with neutrals (~40 collisions/s). If any of the transitions we observe in our spectra are hot-band transitions, that is, transitions from excited vibrational states of the anion, it should be possible to increase the intensity of these transitions by "heating" the ions, thereby increasing the populations in the excited vibrational levels. In an attempt to do this, we have formed the *tert*-butoxyl anion in our experiments in two different ways:

$$(CH_3)_3COH + F^- \rightarrow (CH_3)_3CO^- + HF \qquad (12)$$

$$(CH_3)_3COOC(CH_3)_3 \xrightarrow{e^-} (CH_3)_3CO^- + (CH_3)_3CO \qquad (13)$$

As mentioned in the Experimental Section, the reaction of *tert*-butyl alcohol with F^- is nearly thermoneutral.[32] However, under the conditions of our experiment, dissociative electron impact on di-*tert*-butyl peroxide could leave the *tert*-butoxyl ion with as much as 40 kcal/mol of excess energy. The photodetachment cross section determined by the experiment on this "hot" *tert*-butoxyl anion is identical in the threshold region with our experiment with F^- and *tert*-butyl alcohol. Unless the ions fortuitously have the same amount of excess vibra-

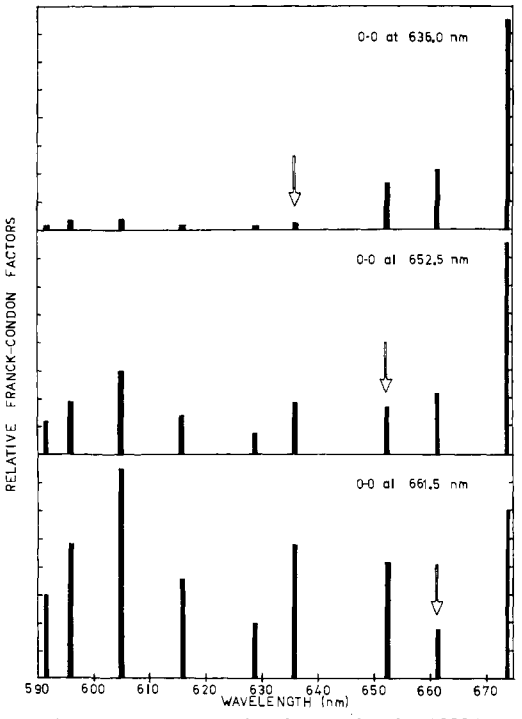

Figure 5. Estimated Franck-Condon factors for the $(CH_3)_3CO^- \rightarrow (CH_3)_3CO + e^-$ transition.

tional energy in each case, we feel that the ions have the opportunity to thermalize in the ICR cell and any hot bands in the spectra are due to thermal vibrational populations in the anions.

Methoxyl. Since the lowest frequency vibrational mode in CH_3O^- is greater than 1000 cm^{-1},[33] the population of excited methoxyl anions should be very small at 300 K. Thus, we can take the photodetachment onset to be an upper limit to the electron affinity of CH_3O. We have previously found[7] that the threshold energy is best determined by subtracting half the monochromator bandwidth from the wavelength of the first nonzero data point. This analysis gives a threshold of 780 nm and $EA(CH_3O) \leq 1.59 \pm 0.04$ eV. However, while the geometry change for the transition $CH_3O^- \rightarrow CH_3O$ is probably responsible for a spreading out of the photodetachment transition intensity and the resulting linear rise in the cross section, the 0-0 transition should be strong enough to be observed and we can take $EA(CH_3O) = 1.59 \pm 0.04$ eV.

***tert*-Butoxyl.** In contrast to methoxyl anion, *tert*-butoxyl has a number of low-frequency vibrational modes with appreciable population at 300 K (a 400-cm^{-1} mode will be 12% populated at this temperature). Given the transition intensities for the various vibronic transitions in the *tert*-butoxyl cross section (Table I), we may pick a particular transition as the 0-0 transition and then estimate the Franck-Condon factors that would give rise to the observed intensities. The results of such a calculation are shown in Figure 5. The top graph shows the calculated Franck-Condon factors if the transition at 636.0 nm is chosen as the adiabatic transition. For a diatomic, the Franck-Condon factors should be approximately the same for the $v'' = n \rightarrow v' = n + m$ and $v'' = n + m \rightarrow v' = n$ transitions. To a first approximation, we should expect the same symmetry about the 0-0 transition for polyatomic Franck-Condon factors. This is clearly not the situation for the top case. The lower two graphs show the relative Franck-Condon factors if the 0-0 transition is chosen at 652.5 or 661.5 nm. In each of these cases, the Franck-Condon factors are essentially symmetric about the adiabatic transition. Although the latter case may be the better choice, we feel that either of these two transitions can be chosen as the 0-0. Therefore, $EA(Me_3CO) = 1.87 \pm 0.01$ or 1.90 ± 0.01 eV. This result is in agreement with a recent determination by Lineberger and co-workers by the method of photoelectron spectroscopy.[34]

Table III. Calculated RO-H Bond Strengths

	EA, eV	DH[a], kcal/mol[a]
MeO	1.59 ± 0.04	101.3 ± 1.0
$(Me)_3CO$	1.90 ± 0.01	102.8 ± 1.0
	1.87 ± 0.01	102.1 ± 1.0
$(Me)_3CH_2CO$	1.93 ± 0.06	102.2 ± 1.4

[a] $DH°(A\text{-}H) = EA(A) + \Delta H°_{298}(AH \rightarrow A^- + H^+) - IP(H)$.

Neopentoxyl. Owing to the fact that no vibronic transitions can be resolved from 645-680 nm even though the cross section is nonzero in this region, a Franck-Condon factor analysis such as that used for *tert*-butoxyl was not attempted for this ion. Instead, the first strong transition at 642 nm is chosen as the 0-0 and larger error bars are assigned to the resulting electron affinity: $EA(Me_3CCH_2O) = 1.93 \pm 0.06$ eV.

D. Thermochemistry. A summary of the results of our experiments on alkoxyl anions is given in Table III. By employing an appropriate thermochemical cycle and the gas-phase acidities of the aliphatic alcohols[35a] we can calculate the RO-H bond strengths for these alcohols with the formula

$$DH^0(RO\text{-}H) = \Delta H°_{298}(ROH \rightarrow RO^- + H^+) + EA(RO\cdot) - IP(H) \quad (14)$$

These results are shown in Table III. As estimated by Benson from gas kinetic measurements,[36] these bond strengths are essentially constant for the aliphatic alcohols studied. However, the bond strengths we have determined are consistently lower by 2 kcal/mol than those estimated by Benson. If our EAs are correct, it would appear that there is either a systematic error in the acidity determinations or the bond strength determinations.[35b] To remove a discrepancy of this size for *tert*-butoxyl anion, we would have to choose the top case of Figure 5 as the 0-0; this corresponds to a vibrational temperature of approximately 1000 K for the *tert*-butoxyl ions in the ICR cell which appears inconsistent with our results.

Substituent Effects. The stabilizing effect of alkyl groups in alkoxyl anions was first considered by Brauman and Blair when they determined the gas-phase acidity order neopentyl alcohol > *tert*-butyl alcohol > ethanol > methanol.[37] Equation 15 shows the semiclassical ion-induced dipole interaction suggested to explain the trend in alkoxyl anion stability:

$$U(r) = -\frac{1}{2}\frac{\alpha e^2}{r^4} \quad (15)$$

where $U(r)$ is the energy and α is the polarizability of a nonpolar alkyl group interacting with a unit charge, e, at a distance, r. In this model, an alkoxyl anion is viewed as a polarizable alkyl group connected to O^-; since larger alkyl groups are more polarizable, eq 15 predicts that they will be more effective at stabilizing the charge on oxygen. This model, however, does not explicitly include electron delocalization, and our alkoxyl anion cross section calculations suggest that this might be important.

A molecular orbital model used in conjunction with Koopmans' theorem can provide a simple picture of alkyl substituent effects. Koopmans' theorem[38] suggests that the energy of the highest occupied molecular orbital (E_{HOMO}) of a closed-shell anion can be taken as a good approximation to $-EA$ of the neutral produced when an electron is removed from this orbital. We note that E_{HOMO} is generally at higher energies for larger neutral molecules. Since $IP \approx -E_{HOMO}$ we predict the trend in ionization potentials of alkyl chlorides: $CH_3Cl > CH_3CH_2Cl > (CH_3)_2CHCl$, in agreement with the observed trend.[39] However, this model does not correctly predict the

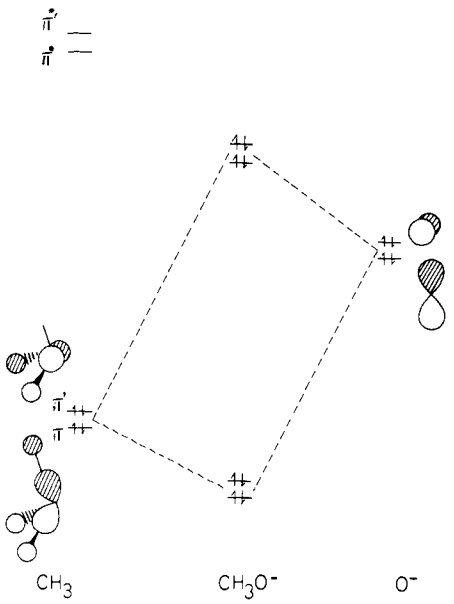

Figure 6. Destabilizing interaction in CH_3O^- between the filled π orbitals on CH_3 and the filled p orbitals on O^-.

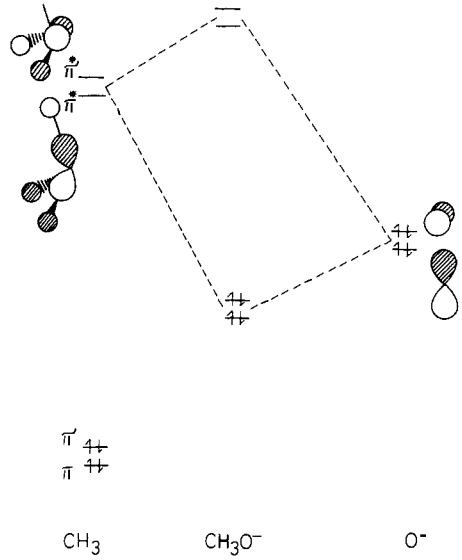

Figure 7. Stabilizing interaction in CH_3O^- between the vacant π^* orbitals on CH_3 and the filled p orbitals on O^-.

alkoxyl radical electron affinities. Since we would also expect E_{HOMO} to be at higher energies for larger negative ions, negative ions with larger alkyl groups would presumably have smaller electron binding energies. This runs contrary to the observed electron affinity trend $Me_3CCH_2O > Me_3CO >$ MeO.

A model better suited to explain the electron affinity trend in the alkoxyl radicals is an extension of that of Hudson, Eisenstein, and Anh[40] and, more recently, Hehre and coworkers.[41] Similar to the ion-induced dipole model, this perturbation picture considers an alkoxyl anion, RO^-, as a combination of an alkyl radical, R, and O^-. As shown for CH_3O^- in Figure 6, the alkyl group π orbitals can mix with the oxygen p orbitals; this interaction is closed shell and destabilizing. However, Figure 7 shows that the mixing of the π^* orbitals on R and the oxygen p orbitals is a stabilizing interaction. This mixing will be stronger and, hence, the stabilizing interaction will be stronger if the R group is increased in size since the π^* orbital will be lower in energy. Of the two types of mixing, the stabilizing interaction appears to be the more important one in alkoxyl negative ions, resulting in a lowering of E_{HOMO} for alkoxyl ions with larger alkyl groups. Thus, the electron affinity trend R'O > RO should be observed if the energy of the lowest unoccupied molecular orbital (E_{LUMO}) of R' is lower than E_{LUMO} of R. Since E_{LUMO} is generally related to alkyl group size, this ordering is expected when R' is larger than R.

The π^*-p orbital mixing which is important in the alkoxyl anions appears not to be the dominant factor in determining the ionization potential trend of the neutral alkyl chlorides. For this case, the p orbitals of chlorine are lower in energy than those on O^- and the π-p repulsive interactions dominate.

Molecular orbital calculations have provided evidence for the importance of the π^*-p orbital interaction in the alkoxyl anions. Both our CNDO/2 calculations and ab initio calculations[30] have found that the electron densities at the hydrogen atoms are larger in CH_3O^- compared to CH_3O. Also, the C-H overlap populations are smaller in the anion than in the neutral. These results indicate that anion stabilization is occurring via hyperconjugative release of electrons onto the alkyl groups where partial occupation of the alkyl π^* orbitals is of prime importance.[42]

The original ion-induced dipole model is a classical consequence of the quantum mechanical model. The polarizability, α, of a molecule is defined as the ratio of the induced electric dipole moment to the strength of the applied electric field. The polarizability can also be related to the second-order Stark effect[43] by the relationship

$$\alpha = \frac{2\omega_2}{E} \tag{16}$$

where

$$\omega_2 = S'_n \frac{|\langle \psi_0 | H' | \psi_n \rangle|^2}{E_0 - E_n} \tag{17}$$

E is the electric field strength, E_0 is the ground-state energy of the molecule, E_n is the energy of the nth excited state of the molecule, ψ_0 is the wave function of the ground electronic state, ψ_n is the wave function of the nth excited state, and S'_n is a summation over the discrete set of wave functions together with an integration over the continuous set of eigenfunctions (the term $n = m$ is omitted and the sum and integration are over n). H' is the perturbation Hamiltonian arising from the influence of the external electric field.

From eq 17 it is clear that larger alkyl groups will give larger negative values for ω_2. This is a consequence of the excited states being closer in energy to the ground state for larger groups (making the denominator smaller) and the number of excited states being greater (making the sum of numerators larger). Thus, it is the presence of low-lying unfilled orbitals that is responsible for the greater polarizability of larger alkyl groups. From the perturbation model description of alkoxyl anion stabilities we would predict, therefore, that the polarizability of alkyl groups should correlate with the stabilities of negative ions.

The perturbation model described above is valid only if Koopmans' theorem is a good approximation. In general, because it neglects the effects of orbital reorganization in anion → neutral transitions, Koopmans' theorem is not a useful tool in predicting anion stabilities. It is not unusual to see large electron correlation effects in closed-shell negative ions,[44] and one would expect that the removal of an electron from a system in which electron correlation is important should result in substantial orbital relaxation.

The magnitude of this relaxation can be determined by comparing the Koopmans' electron affinity of an open-shell molecule (E_{HOMO} of the anion) to the energy difference between an SCF calculation on the neutral molecule and the molecular anion (ΔSCF). The difference $E_{HOMO} - \Delta SCF$ is[44]

over 3 eV for OH^- and is indicative of the problems in applying Koopmans' theorem to negative ions. However, for the series of aliphatic alcohols the RO-H bond dissociation energies are essentially constant implying that there are no stabilizing effects in the alkoxyl radicals which depend on the size of the alkyl groups. This suggests that orbital reorganization will not be the controlling factor of the electron affinity trend in the alkoxyl radicals. Therefore, the trend in E_{HOMO} for the alkoxyl anions should agree with the observed electron affinity trend for the radicals. Although Koopmans' theorem is qualitatively valid for the alkoxyl anions, this is a fortuitous case that could not have been predicted without the RO-H bond strength data.

A comparison of the electron affinities of CH_3O (EA = 1.59 eV) and OH (EA = 1.829 eV)[45] provides an example of the problems in applying Koopmans' theorem to negative ions. As shown above, the π^*-p interaction should stabilize CH_3O^- relative to OH^- where this interaction is not present, making $EA(CH_3O) > EA(OH)$ by Koopmans' theorem (wrong prediction). However, by applying the perturbation model to CH_3O we observe a stabilizing interaction in this system also, if CH_3O is taken to be a combination of CH_3 and an oxygen atom. The oxygen atom p orbitals are lower in energy than those on O^-, and the resulting interaction of a methyl π orbital with a half-filled oxygen p orbital will result in a stabilizing effect in CH_3O which is not present in OH. Evidence that this effect is important lies in the fact that the O-H bond strength in CH_3OH is 15 kcal/mol lower than that of H_2O.[46] Thus, there are stabilizing interactions present in both CH_3O^- and CH_3O not present in either OH^- or OH, and it is impossible to predict from the perturbation model which of the interactions in the methoxyl system will be stronger. Clearly, the stabilizing effect in the methoxyl radical causes Koopmans' theorem to be a poor approximation when comparing the electron affinities of CH_3O and OH due to the different extent of orbital relaxation occurring in CH_3O^-/CH_3O compared to OH^-/OH. This example is representative of the difficulties in using Koopmans' theorem and suggests that it should be used with caution in dealing with negative ions.

Summary

Photodetachment spectroscopy has been applied to three alkoxyl anions, and electron affinities of the corresponding radicals have been determined from the thresholds. Vibrational fine structure can be observed in these spectra when a tunable dye laser is used as a light source. The threshold shapes are calculated and compared to the experimental cross sections. A perturbation model is described which correctly predicts the electron affinity trend of the alkoxyl radicals.

Acknowledgments. We thank Professor W. C. Lineberger and Dr. Paul Engelking at J. I. L. A., Boulder, Colo., for helpful discussions and correspondence. We are grateful to the National Science Foundation for research support and Predoctoral Fellowships to A.H.Z. and B.K.J.

References and Notes

(1) L. M. Branscomb, *Phys. Rev.*, **148**, 11 (1968).
(2) H. Hotop, T. A. Patterson, and W. C. Lineberger, *J. Chem. Phys.*, **60**, 1806 (1974).
(3) M. W. Siegel, R. J. Celotta, J. L. Hall, J. Levine, and R. A. Bennett, *Phys. Rev. Sec. A*, **6**, 607 (1972).
(4) M. W. Siegel, R. J. Celotta, J. L. Hall, J. Levine, and R. A. Bennett, *Phys. Rev. Sect. A*, **6**, 631 (1972).
(5) K. C. Smyth and J. I. Brauman, *J. Chem. Phys.*, **56**, 5993 (1972).
(6) W. C. Lineberger and B. W. Woodward, *Phys. Rev. Lett.*, **25**, 424 (1970).
(7) K. C. Smyth and J. I. Brauman, *J. Chem. Phys.*, **56**, 1132 (1972).
(8) E. Herbst, T. A. Patterson, and W. C. Lineberger, *J. Chem. Phys.*, **61**, 1300 (1974).
(9) K. J. Reed and J. I. Brauman, *J. Am. Chem. Soc.*, **97**, 1625 (1975).
(10) K. C. Smyth and J. I. Brauman, *J. Chem. Phys.*, **56**, 1132 (1972).
(11) K. C. Smyth and J. I. Brauman, *J. Chem. Phys.*, **56**, 4620 (1972).
(12) Pressures were recorded at the Vac Ion Pump; the actual cell pressure may differ from these measured pressures by as much as a factor of 2.
(13) P. L. Hanst and J. G. Calvert, *J. Phys. Chem.*, **63**, 104 (1959).
(14) P. Gray, R. Shaw, and J. C. J. Thynne, *Prog. React. Kinet.*, **4**, 65 (1967).
(15) J. C. J. Thynne, *Org. Mass Spectrom.*, **7**, 899 (1973).
(16) (a) L. von Trepka and H. Neuert, *Z. Naturforsch. A*, **18**, 1295 (1963); (b) B. J. Hauffe, *Z. Phys. Chem. (Frankfurt am Main)*, **85**, 175 (1973).
(17) (a) R. T. McIver and J. S. Miller, *J. Am. Chem. Soc.*, **96**, 4323 (1974); (b) CH_3OH is 1.3 kcal/mol less acidic than the published acidity (R. McIver, private communication).
(18) F^- produced from NF_3 by electron impact has approximately 9 kcal/mol translational energy. J. L. Franklin, *Science*, **193**, 725 (1976).
(19) (a) J. I. Brauman and L. K. Blair, *J. Am. Chem. Soc.*, **92**, 5986 (1970); (b) L. M. Tel, S. Wolfe, and I. G. Csizmadia, *J. Chem. Phys.*, **59**, 4047 (1973); (c) L. Radom, *J. Chem. Soc., Chem. Commun.*, 403 (1974); (d) N. C. Baird, *Can. J. Chem.*, **47**, 2306 (1969); (e) R. B. Hermann, *J. Am. Chem. Soc.*, **92**, 5298 (1970); (f) M. Graffeuil, J.-F. LaBarre, and C. Leibouici, *J. Mol. Struct.*, **23**, 67 (1974).
(20) (a) J. H. Richardson, L. M. Stephenson, and J. I. Brauman, *J. Chem. Phys.*, **59**, 5068 (1973); (b) *ibid.*, **62**, 1580 (1975).
(21) (a) R. C. Dunbar, *J. Am. Chem. Soc.*, **93**, 4354 (1971); (b) *ibid.*, **95**, 6191 (1973).
(22) K. J. Reed, A. H. Zimmerman, and J. I. Brauman, *J. Am. Chem. Soc.*, **99**, 7203 (1977).
(23) K. Jager, M. Simic, and A. Henglein, *Z. Naturforsch. A*, **22**, 961 (1967).
(24) C. M. Reinsch, *Numer. Math.*, **10**, 177 (1967); **16**, 451 (1971). The program SEVAL (G. E. Forsythe, M. A. Malcolm, and C. B. Moler, "Computer Methods for Mathematical Computations", Prentice-Hall, Englewood Cliffs, N.J., 1977, p 76) was used to calculate the cubic spline functions. The program was modified slightly such that the spline could be evaluated at any point. The program SMOOTH (Argonne National Laboratory Applied Mathematics Division Program E350S) was used to smooth the calculated spline.
(25) E. P. Wigner, *Phys. Rev.*, **73**, 1002 (1948).
(26) K. J. Reed, A. H. Zimmerman, H. C. Andersen, and J. I. Brauman, *J. Chem. Phys.*, **64**, 1368 (1976).
(27) The program CNINDO, Program 141, Quantum Chemistry Program Exchange, Department of Chemistry, Indiana University, Bloomington, Ind., was used for the calculations.
(28) The weak nature of the dipole and induced dipole forces binding the outermost electron in a negative ion ensures that this electron will occupy more spatially diffuse regions than in neutrals where the outermost electrons are bound in a screened Coulomb potential. See, for example, E. Clementi and A. D. McLean, *Phys. Rev.*, **133**, 419 (1964).
(29) D. S. Burch, S. J. Smith, and L. M. Branscomb, *Phys. Rev.*, **112**, 171 (1958).
(30) D. R. Yarkony, H. F. Schaeffer, and S. Rothenberg, *J. Am. Chem. Soc.*, **96**, 656 (1974).
(31) H. A. Jahn and E. Teller, *Proc. R. Soc. London, Ser. A*, **161**, 220 (1937).
(32) Considering the translational energy of the fluoride ion (see ref 18) reaction 12 could be at most 8–9 kcal/mol exothermic.
(33) The HCH bend in methyl fluoride is 1196 cm^{-1}. G. Herzberg, "Infrared and Raman Spectra of Polyatomic Molecules", Van Nostrand, Princeton, N.J., 1945, p. 315.
(34) The photoelectron experiment gave a preliminary electron affinity of 1.912 eV.
(35) (a) J. E. Bartmess and R. T. McIver, Jr., *J. Am. Chem. Soc.*, **99**, 4163 (1977); see also ref 17a. (b) A recent reexamination of these acidities by McIver indicates that the original ΔH°_{298} ($ROH \rightarrow RO^- + H^+$) values might be slightly too small owing to a low estimate of the temperature in the ICR cell (R. T. Iver, Jr., paper presented at the 175th National Meeting of the American Chemical Society, Anaheim, Calif., March 1978).
(36) S. W. Benson and R. Shaw, *Adv. Chem. Ser.*, **No. 75**, 288 (1968).
(37) J. I. Brauman and L. K. Blair, *J. Am. Chem. Soc.*, **92**, 5986 (1970).
(38) T. Koopmans, *Physica (Utrecht)*, **1**, 104 (1934).
(39) (a) K. Watanabe, *J. Chem. Phys.*, **26**, 542 (1957); (b) K. Watanabe, T. Kanayama, and J. Mottl, *J. Quant. Spectrosc. Radiat. Transfer*, **2**, 369 (1962).
(40) R. F. Hudson, O. Eisenstein, and N. T. Anh, *Tetrahedron*, **31**, 751 (1975).
(41) D. J. DeFrees, J. E. Bartmess, J. K. Kim, R. T. McIver, and W. J. Hehre, *J. Am. Chem. Soc.*, **99**, 6451 (1977).
(42) See also T. P. Lewis, *Tetrahedron*, **25**, 4117 (1969); W. J. Hehre and J. A. Pople, *Tetrahedron Lett.*, **34**, 2959 (1970); P. H. Owens, R. A. Wolf, and A. Streitwieser, Jr., *Ibid.*, **38**, 3385 (1970).
(43) L. I. Schiff, "Quantum Mechanics", McGraw-Hill, New York, N.Y., 1968, p 265.
(44) J. Simons, *Annu. Rev. Phys. Chem.*, **28**, 15 (1977).
(45) R. J. Celotta, R. A. Bennett, and J. L. Hall, *J. Chem. Phys.*, **60**, 1740 (1974).
(46) J. A. Kerr, *Chem. Rev.*, **66**, 465 (1966).